［溶接学会論文集　第 35 巻　第 2 号　p. 38s-41s（2017）］

Simulation of Flux Melting Process during a SAW by DEM-ISPH Hybrid Method*

by Hisaya Komen**, Masaya Shigeta***, Manabu Tanaka***, Mitsuyoshi Nakatani**** and Yohei Abe****

Simulation of molten flux flow during submerged arc welding was carried out by a hybrid method using Discrete Element Method and Incompressible Smoothed Particle Hydrodynamics method. As a result, flux melting process was calculated with time evolution. Moreover, it was also simulated that molten flux was re-solidified at a backward of a heat source. In this simulation, the average thickness of this slag at z = 5.0±0.25 mm (the center of the wire in the z direction) was estimated to be 4.8 mm. These results showed that the potential and the usefulness of this hybrid method to simulate the flux melting during SAW.

Key Words: Submerged arc welding, Flux, Slag, DEM, Particle method

1. Introduction

Submerged Arc Welding (SAW) is a welding process which is applied to large structures such as buildings, ships, bridges and so on, because this process can obtain deep penetration due to its high welding efficiency. During this welding, the arc plasma, the molten metal and the weld bead are covered with flux powders. Therefore, it is hard to observe welding phenomena and some research groups are trying to visualize those phenomena. For example, Reisgen et al. investigated the molten metal droplet transfer during SAW[1]. In their study, the heat source moved along with a wall which was made of heatproof glass. They observed the transfer processes through the wall. Moreover, they inserted a ceramic tube in the flux. The arc plasma was captured by a high-speed camera through the tube. They also successfully to visualize fluxes around the arc space and the molten metal droplet transfer. On the other hand, to understand SAW phenomena, there are also some studies using computational simulation. Cho et al. investigated the weld pool convection during a SAW[2]. They calculated velocity fields in a weld pool using an arc model which was approximated from experimental data. The penetration depth obtained from their calculation agreed with an experimental result. Meanwhile, Tanaka et al. simulated arc phenomena in a SAW[3]. Although their model was simple and assumed an axial symmetry condition, they calculated the energy balance from a cathode to an anode during welding and indicated that 80% of the emission loss of a plasma is transported to flux around an arc space. However, they did not consider the behavior of flux because it is difficult for traditional grid methods to simulate the behavior of flux powders.

In this study, the hybrid method using a Discrete Element Method (DEM) and an Incompressible Smoothed Particle Hydrodynamics (ISPH) method is developed to simulate the flux melting and slag forming processes simultaneously.

2. Governing equations

2.1 Momentum equations for DEM

According to the Newton's equation of the motion, the velocity of a powder particle a is determined by[4]

$$\frac{D\vec{u}_a}{Dt} = \frac{1}{m_a}\left(-\sum_b k\,(d - |\vec{r}_{ab}|)\overrightarrow{n_n}_{ab} + \sum_b \overrightarrow{F_s}_{ab} + \sum_b \eta\overrightarrow{u'}_{ab}\right) + \vec{g}\,. \quad (1)$$

Here, $\vec{u}$ is the velocity vector of the particle, t is the time, m is the mass of flux, k is the spring constant. In addition, d is the diameter of a particle, $\vec{r}$ is the relative vector, $\overrightarrow{n_n}$ is the normal unit vector, $\overrightarrow{F_s}$ is the friction force vector, η is the damping coefficient, $\overrightarrow{u'}$ is the relative velocity vector at a contact point of particles and $\vec{g}$ is the acceleration vector of gravity. The angular velocity of a particle a is described as

$$\frac{D\vec{\omega}_a}{Dt} = \frac{1}{I_a}\sum_b \overrightarrow{F_s}_{ab} \times \vec{r}_{ac}, \quad (2)$$

where $\vec{\omega}$ is the angular velocity vector, I is the inertia moment.

*Received: 2016.10.17
**Student Member, Joining and Welding Research Institute Osaka University
***Member, Joining and Welding Research Institute Osaka University
****Member, Hitachi Zosen corporation

2.2 Momentum equation for ISPH

The velocity of a liquid particle a is determined by the Navier-Stokes equation, which is written as[5)]

$$\frac{D\vec{u}_a}{Dt} = -\sum_b m_b\left(\frac{p_a}{{\rho_a}^2}+\frac{p_b}{{\rho_b}^2}\right)\nabla_a W_{ab} + \frac{2dim}{\lambda_a n_a \rho_a}\sum_b \frac{\mu_a+\mu_b}{2}(\vec{u}_b-\vec{u}_a)W_{ab} - \beta(T_a-T_0)\vec{g}\,. \quad (3)$$

Here, p is the pressure, ρ is the density, W is the kernel function, dim is the dimension number and λ is the parameter [6)]. n is the number density, μ is the viscosity coefficient, β is the coefficient of the volume expansion, T is the temperature and T_0 is the reference temperature. In this simulation, the density homogenizing algorithm which is developed by Okachi et al.[7)] is used to express the incompressible flow using the pressure gradient term in Eq. (3).

2.3 Energy transfer equation

Temperature changes of all particles are determined by the energy transfer equation, which is described as

$$\frac{DT_a}{Dt} = \frac{2dim}{\lambda_a n_a \rho_a {C_p}_a}\sum_{a\cup b\notin flux}\frac{\kappa_a+\kappa_b}{2}(T_b-T_a)W_{ab} + \frac{1}{\rho_a V_a {C_p}_a}\sum_{a,b\in flux}(H_c+H_g)(T_b-T_a) + \frac{Q_a}{\rho_a {C_p}_a} \quad (4)$$

C_p is the specific heat, κ is the thermal conductivity, V is the volume of particle, H_c is the contact conductance, H_g is the gas conductance and Q is the heat generation rate[8)]. This heat generation rate includes the heating by radiation from an arc plasma and the emission loss on surfaces of melted flux, slag and base metal. The radiative heating is calculated based on the assumption in which N_a particles with temperatures higher than the boiling point (2500 K) release 1.82×10^9 W/(m^{3}sr) per 1 particle. In this calculation, total radiation energy is given to N particles whose temperatures are lower than the boiling point, which contact with the isothermal surface of the boiling point.

3. Computational conditions

Figure 1 shows the vertical section of the computational domain. The box (10 mm×20 mm×50 mm) which consists of four side walls and one base metal plate is filled up by flux particles. The wire with the diameter of 1.5 mm consists of solid particles. This wire moves at 5 mm/s in the travel direction. Moreover, metal droplet transfer phenomena are not considered and particles comprising the wire move only in the travel direction. However, in order to consider the effect of the wire feed, -6.0 m/min is given to the wire particles in y direction when the velocities of particles are calculated using Eq. (1) and Eq. (3). Arc particles are selected from the domain between the tip of the wire and the surface of the base metal in the y direction and within 0.75 mm from the center of the wire in the radial direction. These arc particles also move at -5 mm/s with the wire in the travel direction. This study adapts several assumptions as follows. In SPH method, particles cannot express continuous body when number of liquid particles is low. Therefore, particles do not move immediately when the particles change their layer from solid to liquid. During this period, neither the wire nor arc particles move. When 150 particles change their layer from solid to liquid, the motions of liquid particles start. Then, the wire and arc particles also start to move. In addition, the formation of the weld bead whose height is about 1.0 mm starts automatically after the heat source passed. Moreover, heat conductivities of the molten flux and the re-solidified slag are assumed to be three times as large as that of flux powders. The latent heat is considered only for the base metal. So, the latent heat affects only the temperature change of the base metal. When the temperature of the base metal particle reaches the melting point, the temperature change of the particle temporarily stops. After the particle gains the latent heat, the temperature starts to change again. However, the phase change of the base metal and the gasification of the molten flux are not considered. Table 1 shows the other computational conditions.

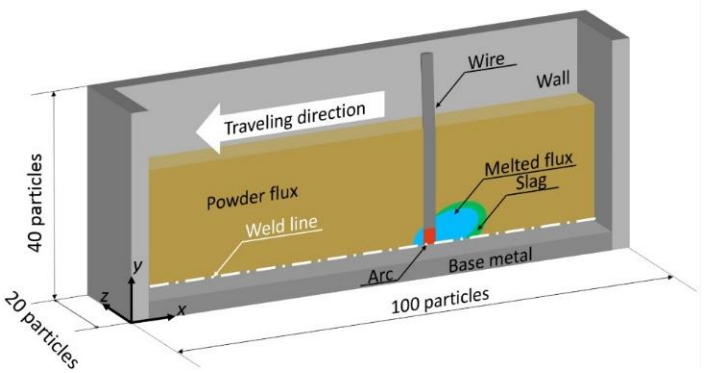

Fig. 1 Schematic illustration of the vertical section of the computational domain.

Table 1 Computational conditions for the SAW model.

Time step	1.0×10^{-4} s
Diameter of particles	ϕ 0.5 mm
Density of flux	3230 kg/m^3
Constant of spring	100 N/m
Melting point	flux: 1486 K
	base metal: 1750 K
Heat conductivity	flux: 4.0 W/(m·K)
	Arc: 2.4 W/(m·K)
	Base metal: 30.0
	~73.0 W/(m·K)
Viscosity	4.0×10^{-3} Pa·s
Coefficient of friction	0.1

4. Results and discussion

Figure 2 shows temperature distribution and particle property distribution at each time. Both of distributions show the vertical cross-section along with the weld line. In the temperature distribution, particles in gray color represent those with temperatures that are lower than the melting point, while blue and red particles show those with temperatures that are higher than the melting point. In the particle property distribution, a base metal and walls are colored by gray and a wire is colored by dark gray. Moreover, red, blue, yellow and green particles show arc, melted flux, powder flux and re-solidified slag, respectively. The powder fluxes are heated by arc particles with time evolution, and fluid is started to move around t = 0.4 s (Figure 2 (a)). After the heat source passed, the melted fluxes are re-solidified gradually from the interface which contacts with powder fluxes (Figure 2 (b)). Finally, a re-solidified slag is formed on a weld bead (Figure 2 (c)). These results showed that the flux melting and slag forming processes are able to be simulated using this hybrid method.

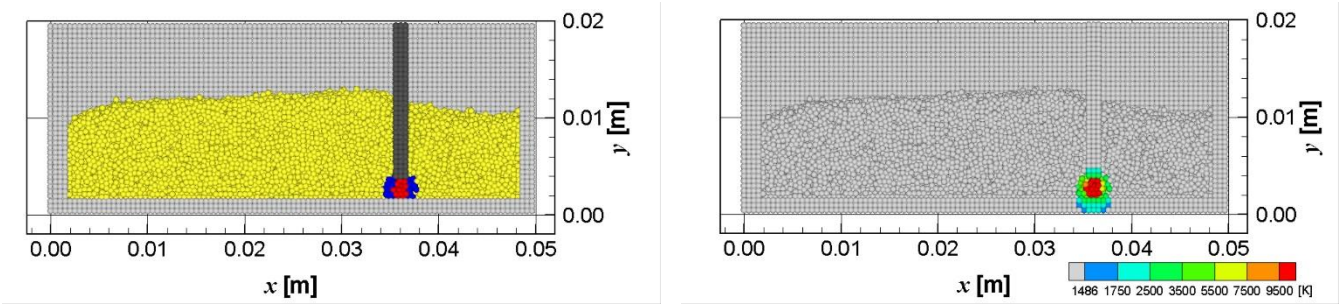

(a) t = 0.4 s

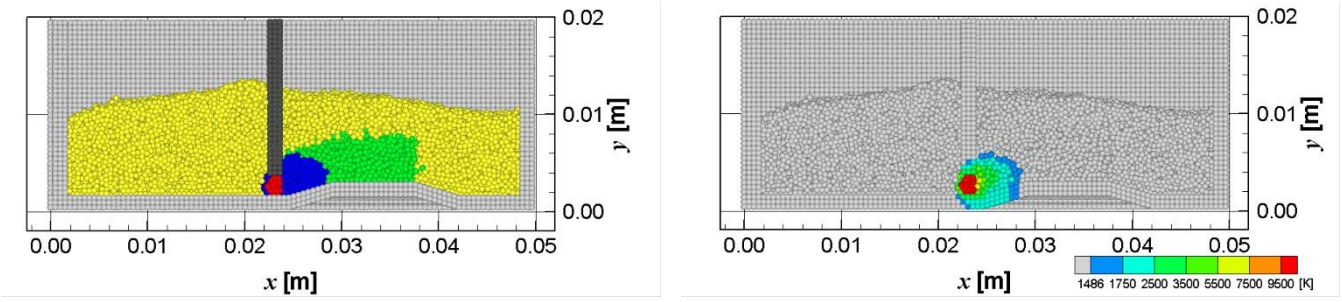

(b) t = 3.0 s

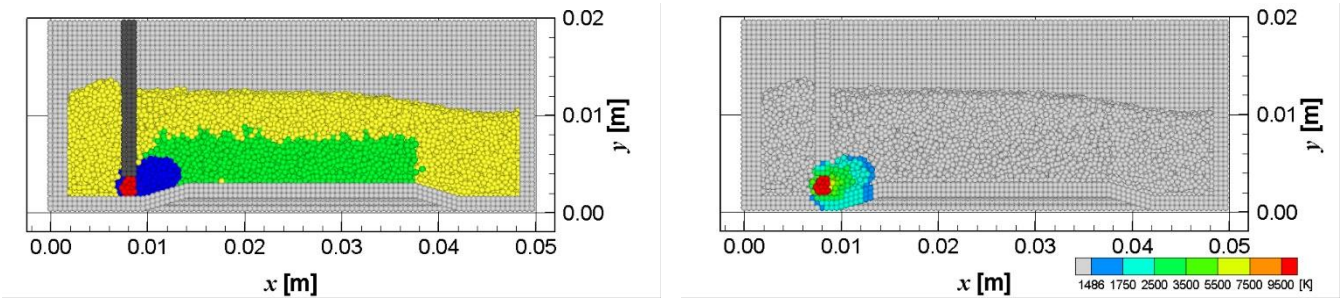

(c) t = 6.0 s

Fig. 2 Vertical sections of Temperature distribution (left) and particle property distribution (right) at the center of the wire.

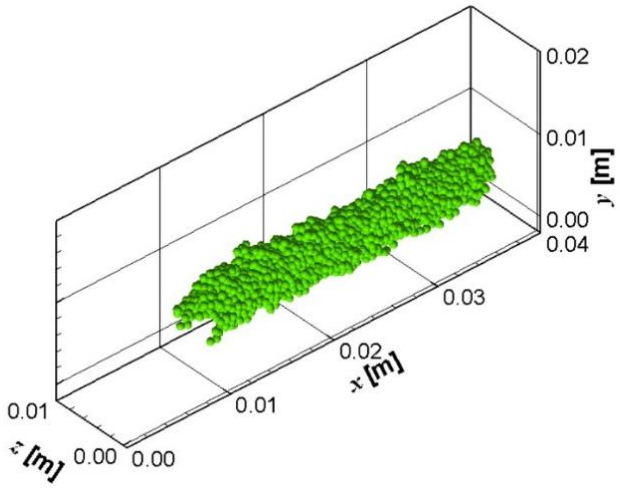

Fig. 3 Slag appearance at t = 6.0 s.

Moreover, some phenomena that increases the flux height in front of a wire and decreases the flux height behind the wire are successfully simulated, which cannot be simulated by traditional grid methods. On the other hand, there are some rooms to be improved in this model. For example, shape of a powder particle in this model is assumed to be a perfect sphere expressed by one particle to reduce the computational costs. However, shapes of actual flux powder particles are more complex. So, although movements of powders in this model are determined by the Newton's equation of motion, some effects acting on the powder such as friction and rotation are different from actual fluxes. To solve this problem, an additional computational model[9] which can express the shape of actual flux powder is should be introduced.

Figure 3 shows the slag appearance at t = 6.0 s. In this simulation, the average thickness of this slag at z = 5.0±0.25 mm (the center of the wire in the z direction) was estimated to be 4.8 mm.

5. Conclusions

A hybrid method using a DEM and an ISPH method was developed to simulate the behaviors of flux powders and the melted flux. The conclusions of this study are summarized as follows:

(1) The flux melting and slag forming processes with the time evolution were simulated.
(2) The DEM-ISPH hybrid method could simulate momentums of powders and the liquid at the same time.
(3) The average thickness of the slag at z = 5.0±0.25 mm was estimated to be 4.8 mm.

Therefore, this study showed that the potential and the usefulness of this hybrid method to simulate the flux melting during SAW. As a future work, the coupling simulation using this model and the weld pool convection model[4] will be conducted to clarify the mechanism of the slag inclusion and predict the penetration shape of the base metal.

References

1) Reisgen et al.: Analysis of the submerged arc in comparison between a pulsed and non-pulsed process, Welding in the World, Vol. 60, No. 4 (2016), pp. 703-711.
2) Cho et al.: Analysis of submerged arc welding process by three-dimensional computational fluid dynamics simulations, Journal of Material Processing Technology 213 (2013), pp. 2278-2291.
3) Tanaka et al.: A Simplified Numerical Model of Submerged Arc Welding, 68th IIW Annual Assembly and International Conference, (2015), Doc. 212-1376-15.
4) Komen et al.: Incompressible SPH Simulation of Molten Metal Droplet Transfer and Weld Pool Convection during GMA Welding, 69th IIW Annual Assembly and International Conference, (2016), Doc. 212-1431-16.
5) Shigeto et al.: GPU Accelerated Simulation for Discrete Element Method, Journal of the Society of Powder Technology, Vol. 45, No. 11 (2008), pp. 758-765.
6) Koshizuka et al.: Moving-particle semi-implicit method for fragmentation of incompressible fluid, Nuclear science and engineering, Vol. 123, No. 3 (1996), pp. 421-434.
7) Okachi et al.: SPH Simulation of Pulsating Pipe Flow at a Junction, 1st International Symposium on Advanced Fluid Information, (2001), pp. 388-391.
8) Vargas and McCarthy: Conductivity of granular media with stagnant interstitial fluids via thermal particle dynamics simulation, International Journal of Heat and Mass Transfer, Vol. 45, (2002), pp. 4847-4856.
9) Iwamoto et al.: 3D SPH-DEM SIMULATION OF TSUNAMI OVERFLOW EXPERIMENT USING GPGPU, Journal of Japan Society of Civil Engineers, Ser. A1 (Structural Engineering & Earthquake Engineering (SE/EE)), Vol. 70, No. 4 (2014), pp. I_295-I_303 (in Japanese).